Structural Basis for Conserved Regulation and Adaptation of the Signal Recognition Particle Targeting Complex

Klemens Wild [1,†], Gert Bange [1,†], Domantas Motiejunas [2], Judith Kribelbauer [1], Astrid Hendricks [1], Bernd Segnitz [1], Rebecca C. Wade [2,3] and Irmgard Sinning [1]

*1 - **Heidelberg University Biochemistry Center (BZH),** INF 328, D-69120 Heidelberg, Germany*
*2 - **Molecular and Cellular Modeling Group,** Heidelberg Institute for Theoretical Studies (HITS), Schloss-Wolfsbrunnenweg 35, D-69118 Heidelberg, Germany*
*3 - **Zentrum für Molekulare Biologie der Universität Heidelberg,** DKFZ-ZMBH Alliance, INF 282, 69120 Heidelberg, Germany*

***Correspondence to Irmgard Sinning:** Heidelberg University Biochemistry Center, Im Neuenheimer Feld 328, D-69120 Heidelberg, Germany. irmi.sinning@bzh.uni-heidelberg.de*
http://dx.doi.org/10.1016/j.jmb.2016.05.015
Edited by Georg Schulz

Abstract

The signal recognition particle (SRP) is a ribonucleoprotein complex with a key role in targeting and insertion of membrane proteins. The two SRP GTPases, SRP54 (Ffh in bacteria) and FtsY (SRα in eukaryotes), form the core of the targeting complex (TC) regulating the SRP cycle. The architecture of the TC and its stimulation by RNA has been described for the bacterial SRP system while this information is lacking for other domains of life. Here, we present the crystal structures of the GTPase heterodimers of archaeal (*Sulfolobus solfataricus*), eukaryotic (*Homo sapiens*), and chloroplast (*Arabidopsis thaliana*) SRP systems. The comprehensive structural comparison combined with Brownian dynamics simulations of TC formation allows for the description of the general blueprint and of specific adaptations of the quasi-symmetric heterodimer. Our work defines conserved external nucleotide-binding sites for SRP GTPase activation by RNA. Structural analyses of the GDP-bound, post-hydrolysis states reveal a conserved, magnesium-sensitive switch within the I-box. Overall, we provide a general model for SRP cycle regulation by RNA.

© 2016 Elsevier Ltd. All rights reserved.

Introduction

Protein targeting is a vital process for all living organisms and eukaryotic organelles like chloroplasts. Co-translational targeting of secretory and membrane proteins is mediated by the universally conserved signal recognition particle (SRP) [1] (Fig. 1). SRP and its receptor (FtsY in bacteria/archaea, heterodimeric SRαβ in eukaryotes) act as regulatory adaptors between ribosome–nascent chain complexes (RNCs) and the translocation channel (SecYEG in bacteria, Sec61 in eukaryotes) in the target membrane [2]. SRP recognizes N-terminal signal sequences of secretory proteins or signal anchor sequences of membrane proteins, docks the RNCs to vacant translocation channels, and is recycled upon GTP hydrolysis in both the SRP and its receptor.

SRP comprises a conserved core consisting of the SRP GTPase SRP54 (Ffh in bacteria) and its cognate binding site on the SRP RNA (helix 8 in eukaryotes and archaea, domain IV in bacteria) [2]. SRP GTPases form a distinct family within the SIMIBI-class (for SRP, MinD, and BioD) of NTP-binding proteins, which are characterized by the formation of nucleotide-dependent dimers [3,4] and have therefore been classified as GADs (G proteins regulated by nucleotide-dependent dimerization) [5]. SRP GTPases include only the three members, SRP54, FtsY, and FlhF, with the latter playing a central role in flagella biosynthesis [6]. SRP GTPases are multi-domain proteins and, besides the central G domain, contain distinct regulatory domains. They are characterized by a low affinity for GTP (μM range) and their stability in the apo form [7]. The G domain harbors the canonical GTPase fold (including the G1–G5 elements involved in nucleotide binding and hydrolysis) with an SRP GTPase-specific insertion between the G2 and G3 elements (I-box or insertion-box domain).

© 2016 Elsevier Ltd. All rights reserved.

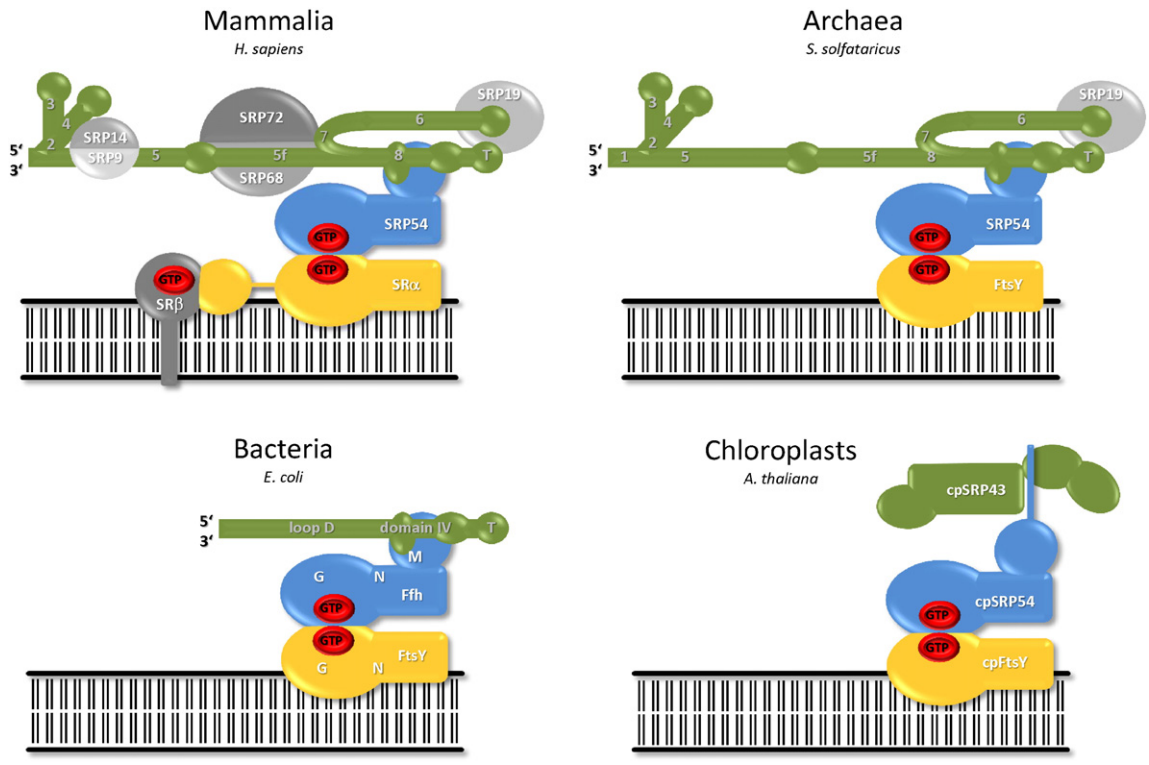

Fig. 1. The Signal Recognition Particle (SRP). Schematic drawings for representative SRP systems of all domains of life and the post-translational chloroplast system, where the cpSRP43 protein replaces SRP RNA (both shown in green). The targeting complex consisting of SRP54/Ffh (blue) and SRα/FtsY (yellow) is generally conserved. Gram-negative bacteria contain a short 4.5S RNA in contrast to the 7S RNA of eukaryotes and archaea. Important features are labeled; NGM: SRP GTPase domains; numbers 1 to 8: RNA helices; 5f/loop D: activating distal sites of SRP RNA; T: conserved tetranucleotide loop of SRP RNA.

The N domain, a bundle of four antiparallel helices, is common to all SRP GTPases. The N and G domains form a conserved structural and functional unit termed the NG domain [8,9]. Detailed studies of the bacterial system suggest that the NG domains of Ffh and FtsY dynamically interact with each other and form the core of the targeting complex (in the following denoted simply by TC). Two distinct TC conformations have been defined to regulate co-translational protein targeting [1]. In an "early" intermediate conformation, Ffh and FtsY interact independently of GTP mainly via the complementary electrostatic properties of their N domains. Cryo-electron microscopy (cryo-EM) studies of the early conformation on the ribosome suggest that the SRP RNA tetraloop closing domain IV of 4.5S RNA ("proximal" site of SRP RNA) contacts the I-box of FtsY [10]. Subsequently, the NG domains of Ffh and FtsY reorganize to form a "closed" conformation in which the two G domains interact in a GTP-dependent manner [11,12], concomitant with the release of the TC from the ribosomal surface, as also observed for the eukaryotic system [13]. Re-localization of the TC, enforced by the translocation channel, has been validated for the bacterial system by recent fluorescence resonance energy transfer (FRET) measurements [14,15] and by high-resolution cryo-EM studies [16,17].

Efficient targeting and translocation is controlled by GTP hydrolysis within the TC, which is also necessary for recycling of the SRP system. The molecular mechanism depends on the activation of an enzyme by RNA. To date, this is a rare case in enzymology and has been described for only a few examples, such as the elongation factor EF-Tu, which is activated by ribosomal RNA upon aminoacyl-tRNA delivery [18]. Structural and FRET studies revealed that in the closed TC conformation, an SRP RNA region "distal" (approx. 90 Å) from the tetraloop is able to bind and stimulate the catalytic GTPase core [3,14,19]. Therefore, SRP RNA assists the SRP cycle by both scaffolding and catalytic activity. Most of our structural knowledge comes from the bacterial SRP systems from the hyperthermophile *Thermus aquaticus* and from *Escherichia coli* [11,12,19,20], which have only a short version of the SRP RNA (4.5S RNA) with slightly more than 100 nucleotides (nts) [2] (Fig. 1). While there are also structural data on individual SRP GTPases from archaea [21], no TC structure is yet available from any other domain of life. The SRPs of

Gram-positive bacteria, archaea, and eukaryotes contain a significantly longer and more complex SRP RNA of about 270 to 500 nts (6S and 7S RNA) [22], whereas in the chloroplasts of higher plants, SRP RNA is absent [23]. Therefore, an intriguing question is how TCs are regulated in these organisms and whether and which structural modifications occurred during evolution. To address these questions, we determined the crystal structures of archaeal, eukaryotic, and higher plant chloroplast TCs.

Results

Crystal structures of archaeal, eukaryotic, and chloroplast TCs

Proteins of the TCs from *Sulfolobus solfataricus* (crenarchaeon), *Homo sapiens* (eukaryote), and *Arabidopsis thaliana* chloroplasts were produced in *E. coli* and stabilized by the non-hydrolysable GTP analogs, 5′-guanylyl-imidodiphosphate (GMPPNP) for the *S. solfataricus* and *H. sapiens* TCs, and β,γ-methyleneguanosine 5′-triphosphate (GMPPCP) for the TC from *A. thaliana*. Crystal structures were determined by molecular replacement at 1.9, 3.2, and 2.5 Å resolution, respectively (Fig. 2a and Table 1). All the TCs are quasi-symmetric heterodimers like their bacterial homologs. Moreover, consistent with their sequence homology (30–40%; Figs. S1 and S2), the overall structural root mean square deviations from the bacterial structures are moderate (approx. 1.5 Å). The specific G elements (G1–G5) and the SRP GTPase typical features, like the I-box and the "ALLEADV", "DARGG", and "RILGMGD" motifs, are present (Figs. 2a, left panel, and S1 and S2). Noticeable deviations between the complexes are mainly found in the length of the α-helices in the N domain (increased in the archaeal and human TCs), in the relative orientation of the N domain to the G domain (20° rotated in the human and archaeal TCs, Fig. 2b), in the conformations of the NG domain linker (Fig. 2c), in the insertions/deletions within surface loops (e.g., for human SRα, Fig. 2a and d), and in the surface charge pattern in the chloroplast TC (see below). All TCs are stabilized in the closed conformation by interactions of their G domains with only minor contributions of the N domains (e.g., for the archaeal TC: 2150 and 600 $Å^2$, respectively). Furthermore, the TC structures have additional external nucleotides and small molecules, like sulfate/phosphate ions and glycerol, bound to distinct sites on their surfaces (Fig. 2a), allowing for a systematic classification of external ligand-binding sites (see below).

The N domains are tightly connected to the G domains, forming the NG domain unit present in all TC structures. However, the interface is not static (nor is the interface to the M domain of SRP54 via the "RILGMGD" motif [24–26], which is not considered here) and is critically involved in the regulation of the targeting process. Helix αN1 is generally part of the bundle in the individual NG domain structures independent of the nucleotide load, but it is found completely detached and not visible in most cases (except in chloroplasts and Ffh in bacteria) in the closed TC structures with bound GTP analogs (Fig. 2b). In FtsY of bacteria and chloroplasts, helix αN1 is preceded by a helical membrane targeting sequence (MTS; not part of the models) [27,28] that is essential for viability in *E. coli* [29]. In *E. coli*, the interaction of the MTS with anionic phospholipids was described to be responsible for a conformational switch within the N domain that is required for TC formation and later activation of the GTPases. Whether such a lipid triggered switch is also present in archaea or chloroplasts is not yet clear. In eukaryotes, membrane attachment of SRα is mediated by the interaction of its N-terminal Longin domain (SRX) with the permanently membrane-anchored, Arf-like GTPase SRβ [30], and MTS-like sequences have not yet been identified.

Formation of the closed TC coincides with a significant rearrangement of the N domains (rotation and translation) with respect to their G domains as described earlier [31]. Namely, the helix following the DARGG motif (Fig. 2a) is "screwed" by one turn enabled by the glycine residues, taking along the N domain and the DARGG motif and thus adjusting the adjacent G4 element for GTP binding. While this mechanism is well established for the bacterial system, we now show that it also applies to archaea but not to chloroplast SR. Eukaryotic SRα lacks the DARGG motif (except the last glycine), and one residue (Asp or Glu) insertion (Fig. S2) results in a bulge and the formation of a salt bridge to the N domain (Fig. 2d). The bulge seems to correlate with the extra 20° rotation of the N *versus* the G domain (Fig. 2b). The structural implications for the N to G domain communication are not yet clear as an unbound SRα structure is still missing.

In summary, the heterodimeric NG domain forms the core of the TC in all domains of life. While most of the regulatory elements are conserved, the differences have a significant impact on the N to G domain communication.

Conservation of the catalytic machinery

Comparative structure analyses of all the different TCs establish the general principle of a composite active center in which two GTP molecules (mimicked by the non-hydrolysable analogs) arrange in a "head-to-tail"-like manner in the interface of the subunits (Fig. 3). This arrangement holds for all SRP GTPases regardless of whether they form homo- or heterodimers [11,12,20,32]. The two nucleotides are close to the twofold symmetry axis between the two subunits,

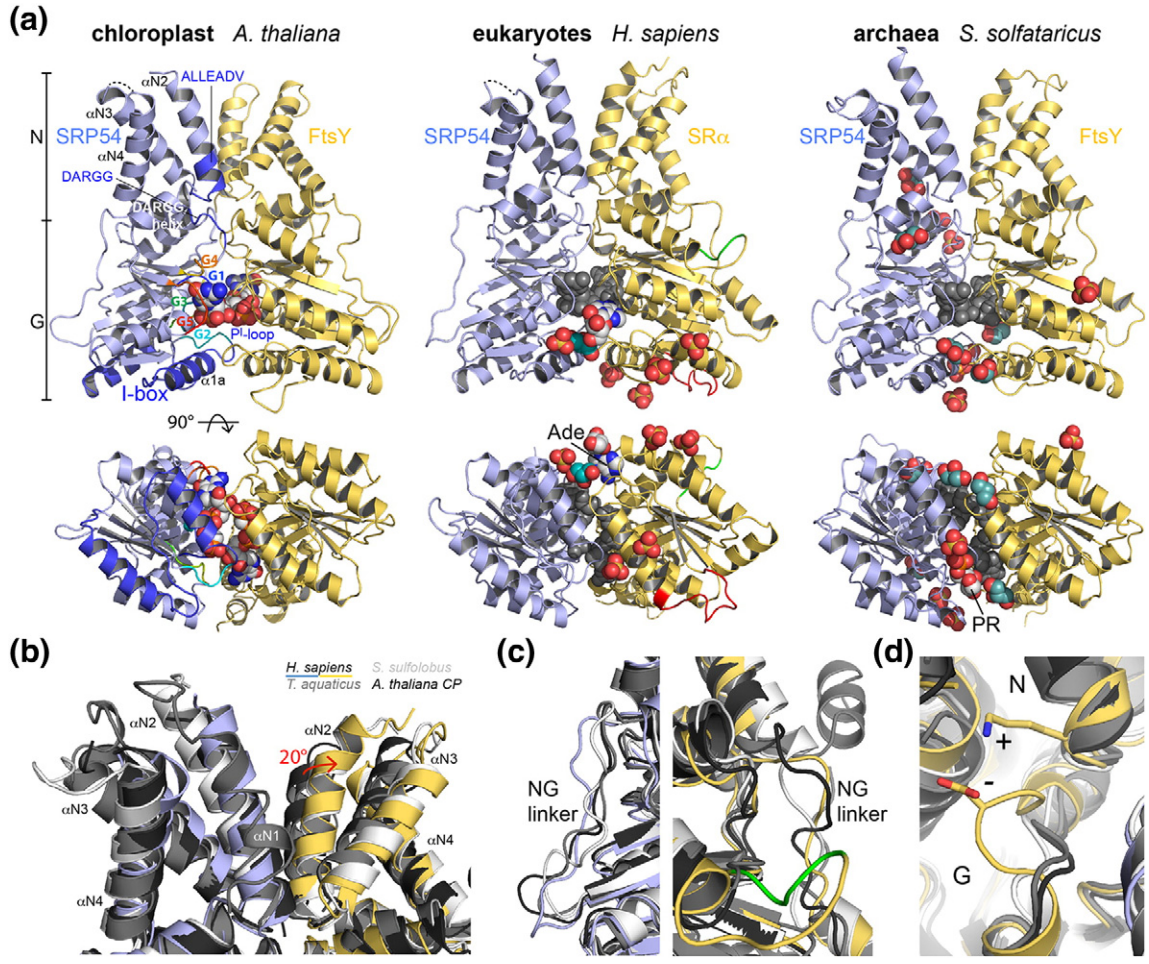

Fig. 2. Overall structures of the targeting complexes. (a) Structures of the chloroplast, human, and archaeal targeting complexes are shown with typical features of SRP GTPase highlighted for chloroplast SRP54 (SRP54: blue; FtsY/SRα: yellow cartoon representations). Helices mentioned in the text are labeled for cpSRP54, and insertions within human SRα are indicated (green, red). Bound ligands are shown as CPK models (spheres). GTP analogs are given in gray for the human and archaeal complexes for distinction from external bound ligands [Ade: adenosine as part of AMP, PR: phosphoribose as part of GMPPNP, and other ligands are sulfates or glycerol molecules (cyan)]. The lower panel shows the TCs viewed from the bottom onto the I-box. (b) The N domains in TC complexes of all domains of life. Helix αN1 is expelled from the helical bundles and is not present in the TCs except for bacterial Ffh. Human and archaeal N domains of the SR are rotated (red arrow) with respect to the chloroplast and bacterial proteins. (c) The N to G domain linkers show different conformations in all species. (d) The insertion in the DARGG motif of SRα in the human TC creates a bulge that is fixed via a salt bridge to the N domain. The color code in C and D is the same as in B.

and the 3′-OH moiety of the ribose in both molecules is hydrogen-bonded to the γ-phosphate *in trans*.

The composite active center consists of two half-sites shaped by the respective G elements G1 to G5 (Fig. 2a, left panel, and Fig. 3). All residues required for nucleotide and magnesium binding and for GTP hydrolysis are highly conserved (Figs. S1 and S2), and side chain conformations are nearly identical in all TC structures. The G1 element (Walker-A motif, P-loop) forms an anion hole for the β-phosphate and has the SIMIBI-typical consensus of GxXGxGKT with an additional (second) glycine, which is necessary due to the close contact in the center of the dimer interface. Residue “X” presents the only conserved sequence asymmetry within the active center. In SRP54/Ffh, it is always a glutamine (Gln), whereas in the SR, it is an asparagine (Asn). This difference introduces asymmetry in the active site as the amide group of the asparagine points toward the catalytic water molecule, and the glutamine always points outward. The conserved threonine (Thr) residue is directly involved in magnesium coordination. The G2 element (DTΦR) serves multiple functions and marks the start of the SRP GTPase-specific I-box. The

Table 1. Data collection and refinement statistics for TC structures

Targeting complex	*S. solfataricus*	*H. sapiens*	*A, thaliana CP*
Resolution range (Å)	37.87–1.90 (1.97–1.90)	76.33–3.20 (3.32– 3.2)	35.73–2.50 (2.59–2.50)
Space group	P21	I23	P21
Unit cell a, b, c (Å)	51.2199.7124.9	241.4241.4241.4	89.9 74.8107.2
α, β, γ (deg)	90 93.0 90	90 90 90	90 91.1 90
Unique reflections	191,335 (17,589)	38,582 (3848)	49,064 (4826)
R_{sym} (%)	6.5 (41.8)	11.8 (45.8)	9.4 (54.0)
Completeness (%)	97.3 (89.7)	99.9 (100.00)	99.3 (99.0)
Mean I/sigma(I)	11.2 (2.0)	11.4 (2.4)	9.5 (2.6)
Redundancy	11.7	3.4 (3.4)	3.7 (3.5)
Wilson B-factor (Å^2)	24.6	61.5	36.4
R-factor (%)	17.3 (28.2)	14.5 (24.5)	16.7 (22.0)
R-free (%)	21.6 (25.6)	19.0 (25.0)	21.4 (27.2)
Number of atoms	19,033	9158	8686
macromolecules	17,402	8828	8402
ligands	417	201	144
water	1214	129	140
RMSD bonds (Å)	0.007	0.010	0.009
RMSD angles (deg)	1.02	1.27	1.24
Ramachandran quality			
Favored (%)	99	98	98
Outliers (%)	0	0	0
Clashscore	8.2	12.4	10.2
Average B-factor (Å^2)	46.0	62.1	45.4
macromolecules	46.3	62.2	45.8
solvent	44.7	41.3	36.0

Statistics for the highest resolution shell are shown in parentheses.

aspartate is involved in magnesium coordination via a water molecule, and the arginine functions as the "arginine finger" (Arg residue stabilizing the transition state in small GTPases [33]) binding to the γ-phosphate *in cis*. The side chains of the G2 arginines of the two GTPases in the TC establish a unique conformational asymmetry in the very center of the complex and are bridged by a water molecule. Due to the different side chain conformations (bent: SR; straight: SRP54/Ffh), this central water molecule is displaced toward the γ-phosphate of the SR. The aromatic residue (Φ) points toward the solvent and, at least for bacterial FtsY, forms the binding platform for a GTPase-activating guanine base of SRP RNA (see below). The G3 element DTAGR follows the I-box with the aspartate being involved in water-mediated magnesium binding and with the glycine forming a nucleotide-dependent hinge with a peptide-flip read-out mechanism. The conserved aspartate residue within the G4 element (TKxD) establishes specificity for guanine nucleotides. The conserved G4 lysine and the G5 element (closing loop, GxGE) form the binding pocket for the guanine of the GTP.

Taken together, the composite catalytic center of the TC is formed by two domains each containing five G elements and is conserved in all domains of life. While twofold symmetry applies to the center, local sequence and conformational asymmetries are observed, which might influence the order of GTP hydrolysis.

Targeting complex formation in archaea

Work on the bacterial system established a mechanism for TC formation proceeding via the nucleotide-free early intermediate [10,34]. This conformation is not stable in solution and could only be stabilized using a fusion protein and in the context of the translating ribosome. The interaction involves long-range electrostatic interactions of opposing charges, which are mainly present in the N-domain helices αN2 and αN3 of both GTPases. With our structural TC dataset in hand, we analyzed the electrostatic properties of SRP54 (or Ffh) and SRα (or FtsY) to investigate whether the charge complementarity of the two GTPases might be conserved. Indeed, all SRP GTPase pairs exhibit overall electrostatic complementarity of their N domains at helices αN2 and αN3 (Fig. 4a), which could facilitate complex formation in a similar fashion to that suggested for the bacterial system. To investigate whether electrostatic steering of N-domain association may contribute to TC formation, we chose the archaeal SRP system to perform Brownian dynamics rigid-body docking simulations subjected to electrostatic intermolecular forces and to varying distance constraints between the two nucleotides (Fig. 4b, upper panel). Upon loosening the distance constraints, more encounter complexes were obtained in which the negatively charged N domain of FtsY is aligned with the positively charged N domain of SRP54 (Fig. 4b, lower panel and

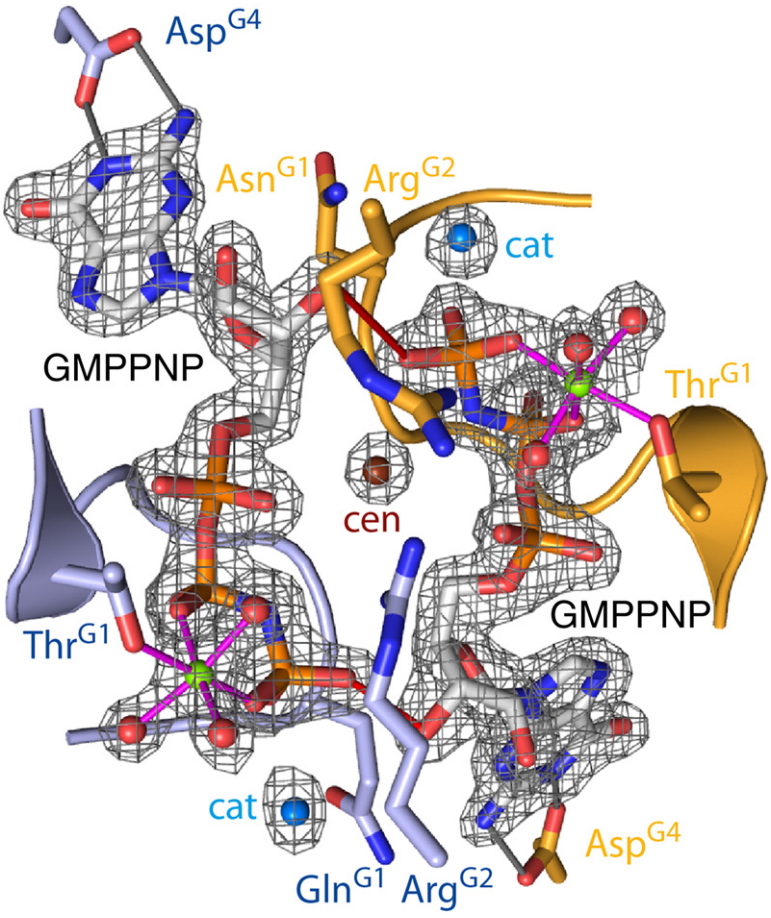

Fig. 3. The conserved composite active center of the TC. The active center of the archaeal TC is shown together with the final 2mFo-DFc electron density (1.0 σ) for the GMPPNP molecules, the octahedral-coordinated magnesium ions (green), and relevant water molecules (cat: catalytic; cen: central). Only a selection of G element residues (in cartoon and stick representation: SRP54: blue; FtsY/SRα: yellow) and hydrogen bonds (solid lines) important for nucleotide binding and magnesium coordination are shown.

Table S1). To dissect the individual contributions to this process, we repeated docking with either the N or the G domains alone. Docking of the individual N domains resulted in encounter complexes with orientations similar to those observed for the full NG domains (Table S2), whereas docking of the G domains resulted in arbitrary orientations (Table S3).

To further investigate the electrostatic steering of complexation, we computationally identified "hot-spot" residues with putatively strong effects on the association rate upon charge variation. In docking simulations of these single-point mutants, the orientation of the encounter complexes was found to be disrupted. The residues with the strongest predicted effects were found to localize in helices αN2 and αN3 of the N domains (Fig. 4c, left panels; SRP54: Lys32 and Lys42; FtsY: Asp108, Glu117). To experimentally validate these observations, we tested alanine and reverse-charge variants of Lys32 and Glu117 for complex formation with their wild-type counterparts. All tested mutants were impaired in complex formation (Fig. 4c, right panels). Consistently, protein variants with reversed charge were more impaired than variants with an alanine exchange. These results support the idea that the electrostatic complementarity of the N domains plays a role in recognition and formation of the early intermediate, at least in the prokaryotic SRP systems.

Targeting complex formation in eukaryotes and chloroplasts

Does TC formation follow a universal mechanism or do the eukaryotic and chloroplast systems work differently? The early conformation is stabilized by the GNRA (N: any nucleotide, R: purine base) tetraloop of SRP RNA in the context of the translating ribosome. Cryo-EM and X-ray studies suggest that the conserved tetraloop of bacterial SRP RNA interacts with a surface area mainly provided by the I-box of FtsY [10,20]. This binding surface includes a critical lysine residue (Lys399 in *E. coli*), which is thought to act as a "transient tether" between SRP RNA and FtsY [35]. Our electrostatic surface analyses reveal that TCs of SRP RNA containing systems exhibit similar properties (Fig. 5a), allowing for the respective interaction of the SRP receptor I-box with

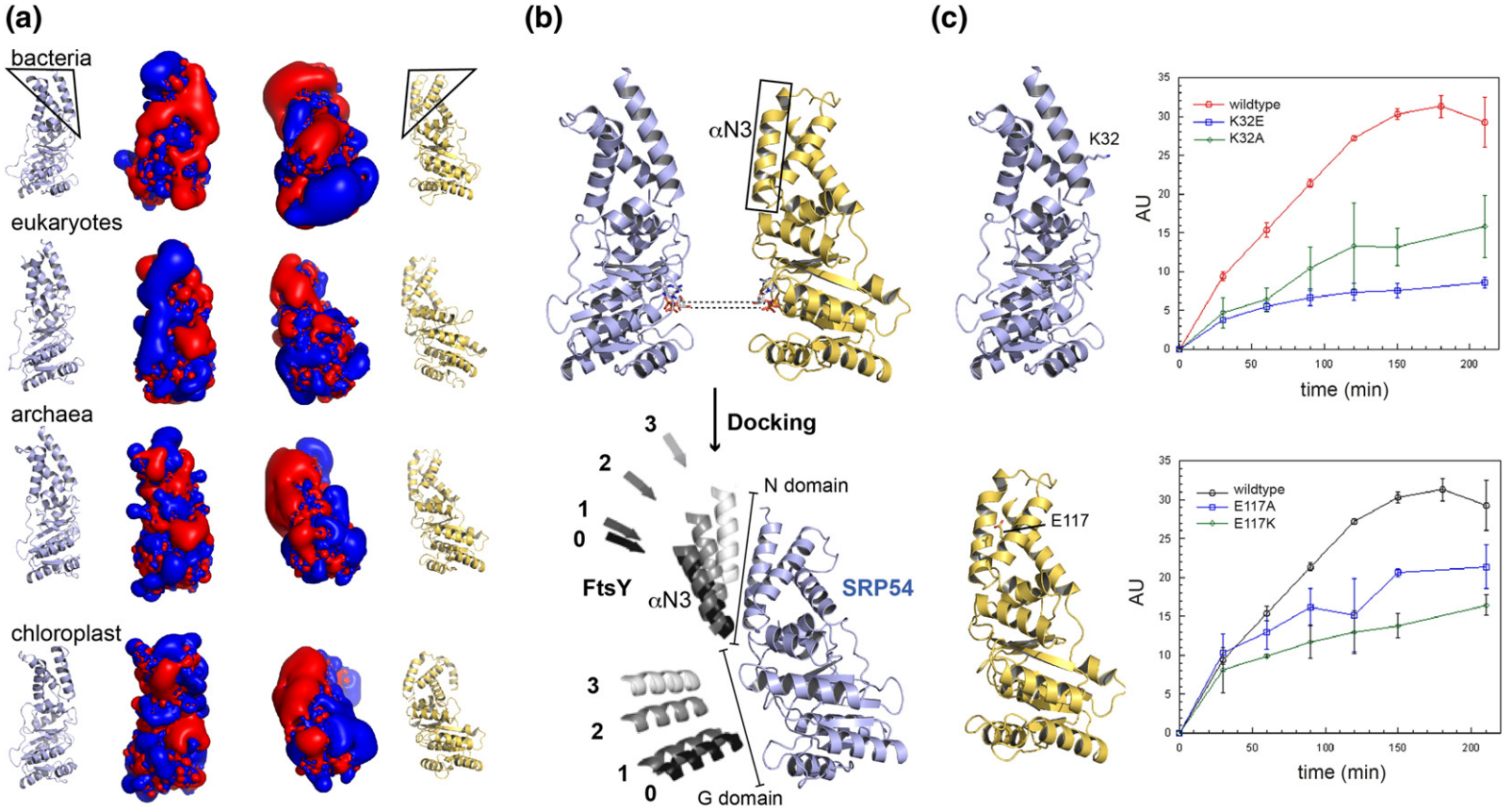

Fig. 4. Formation of the early TC intermediate. (a) Electrostatic isopotential surfaces (±0.5 kT/e, blue: positive, red: negative) for closed TCs from all domains of life. The electrostatic potentials were calculated for the separated NG domains from the structures of the TCs as shown, and orientations and colors are according to Fig. 2 (SRP54: blue; FtsY/SRα: yellow). Helices αN2 and αN3 are indicated by triangles in the bacterial NG domains. (b) Upper panel: Docking of archaeal FtsY to SRP54 was performed with a range of distance constraints between the bound nucleotides, indicated by the dashed lines, in order to investigate the contribution of electrostatic steering to association of FtsY and SRP54. Helix αN3 of FtsY is indicated by the box. Lower panel: The most prominent docking clusters of archaeal FtsY (shades of gray) on SRP54 obtained with different distance constraints (10 Å: "1", 14 Å: "2", and 20 Å: "3") show electrostatic steering of the association of the N domains. The closed conformation in the crystal structure of the TC is labeled "0". Only residues 186–200 (indicative for the G domain) and residues 95–109 (helix αN3, indicative for the N domain) of FtsY are shown for ease of visualization. (c) Impaired complex formation for SRP54 and FtsY N domain charge variants (left panels, mutated residues are indicated) and progression of complex formation monitored over time by size-exclusion chromatography (right panels).

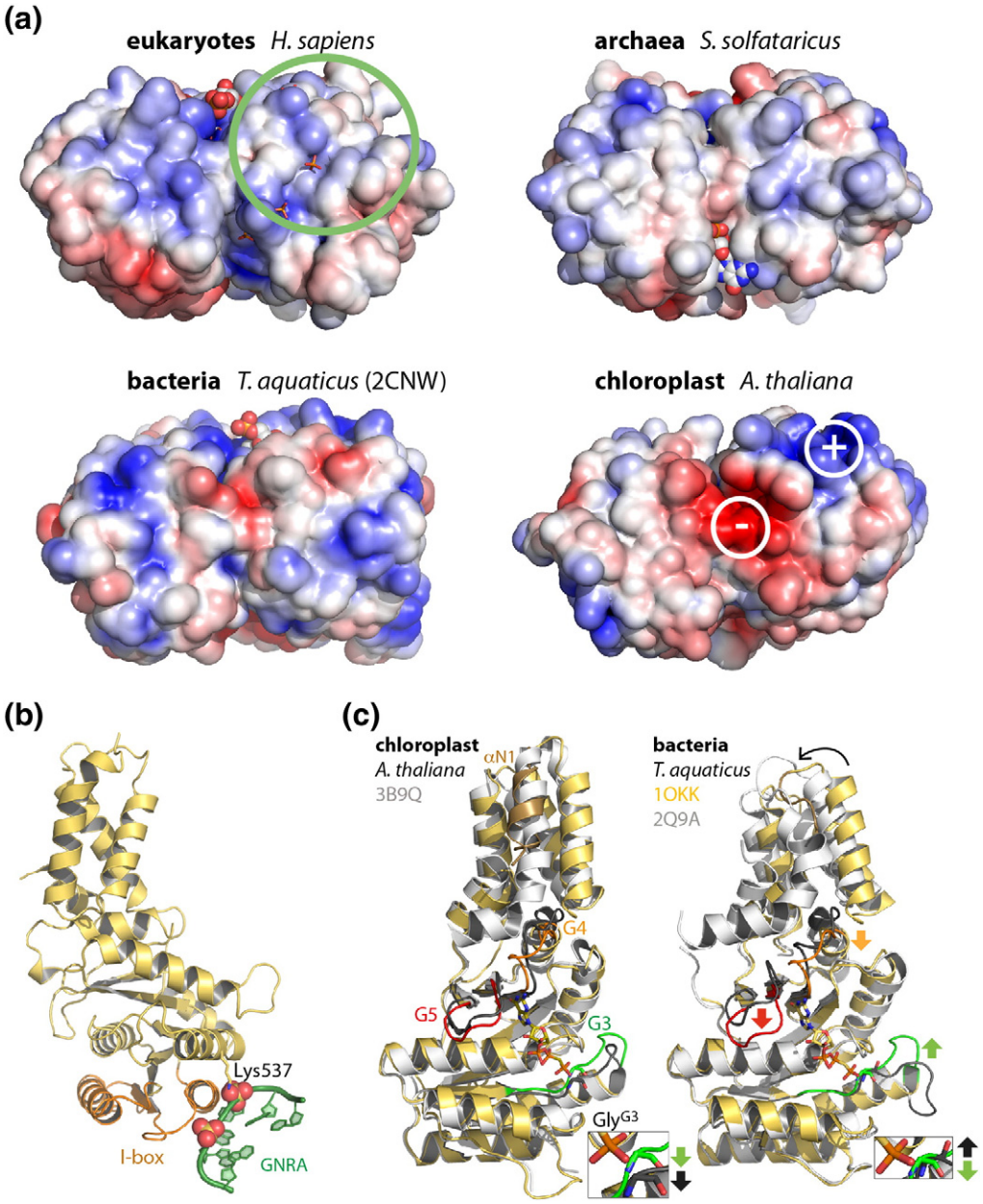

Fig. 5. Stabilization of TC formation. (a) Electrostatic potentials (±5 kT/e, blue: positive, red: negative) mapped on the surfaces of the closed TCs viewed looking onto the I-boxes with bound external nucleotides (spheres) and sulfates (sticks). The SRP RNA-binding region is denoted on the human TC (green circle). The chloroplast TC reveals pronounced charged patches at the I-box interface (negative: "–") and at the lateral side of the cpFtsY I-box (positive: "+"). (b) Overlay of the GNRA tetraloop (PDB ID: 3ZN8) on human SR with bound sulfates. The conserved "tethering lysine" (Lys537) is shown. (c) Details of the pre-organization within cpFtsY. The G3, G4, and G5 elements within the TC (left, colors as in Fig. 2) adopt similar conformations in apo cpFtsY (gray, G elements: black). Helix αN1 of FtsY (gold) is still part of the four-helix bundle. Larger movements of the G elements and N to G rotation (indicated by arrows) are observed in the bacterial systems (right, same color coding). Helix αN1 is not part of the helical bundle in the TC. The insets show magnifications of the peptide geometry and the flip of the G3 glycine (indicated by colored arrows).

SRP RNA in the early conformation. The notion of a conserved binding platform is also supported by the structure of the human TC, where two sulfate ions mimic the tetraloop interaction by binding to the very same sites as the exposed phosphates of the tetraloop in bacterial cryo-EM and X-ray structures [10,20] (Fig. 5b). This binding site also includes the described tethering lysine (Lys537 in human SRα). However, it should be noted that the same area is involved in binding the distal site of bacterial SRP RNA

in the "activated" state of the TC (relocated) and that the sulfate ions could be indicative of a similar relocation in the eukaryotic SRP system (see below).

In the chloroplast TC of higher plants, SRP RNA is absent and "replaced" in the post-translational targeting mode by the cpSRP43 protein [23]. Here, the surface charge distribution is significantly altered (Fig. 5a). Notably, the I-box region next to the dimer interface is highly negatively charged. However, chloroplast FtsY features a highly positively charged patch on the lateral side of the I-box. As the overall shape and charge distribution of cpSRP43 resembles an RNA surface [36], it might as well functionally replace SRP RNA and bind to the positively charged patch. In the structure of cpFtsY from the moss *Physcomitrella patens* [23], this patch is also preserved (Fig. S2). *P. patens* serves as a model system for lower plants, where cpSRP43 and SRP RNA are present simultaneously, although the SRP RNA has already lost its GNRA tetraloop [23].

The differences observed in chloroplast SRP systems call the formation of an early conformation into question. Electrostatic complementarity of the N domains in the chloroplast SRP GTPases would allow for a similar mechanism of TC formation to the canonical, co-translational SRP systems, and biochemical studies reveal that the kinetics of association match the co-translational bacterial system [37]. Comparison of the chloroplast TC with the previously determined cpFtsY structure [28] highlights a conformational pre-organization (Fig. 5c). This pre-organization might prime the protein for efficient nucleotide binding and consequently for complex closure and compensate for the absence of SRP RNA. In detail, the G3 element of the unbound cpFtsY is already positioned as in the closed TC with the conserved glycine having undergone a peptide flip, and nucleotide specificity is significantly higher as reflected by the pre-organization of the G4 (with DARGG) and G5 elements. N to G domain movement during complex formation is reduced in cpFtsY when compared to FtsYs from SRP RNA-containing systems. Finally, in contrast to all other TCs, helix αN1 is not detached from the N domain. However, despite these structural differences to canonical SRP systems, it cannot be excluded that in co- and post-translational targeting, cpSRP43 or another component assists in stabilizing the early conformation in a similar way to the SRP RNA.

SRP RNA-driven activation of GTP hydrolysis

Once the early TC is formed on the RNC, it detaches from its tetraloop-binding site [13,19]. As described for bacteria, the TC subsequently relocates to the distal site (loop D) of SRP RNA (Fig. S3A), providing room for the translocation channel on the ribosomal tunnel exit to receive the signal peptide and to translocate the nascent chain [19,20]. Peculiar to the SRP system is the mechanism of GTPase activation by RNA. The mechanism is now well established for the bacterial system [38], but whether it applies to the other domains of life is not clear.

The composite active center includes two nucleotides, and thus, each TC contains two active half-sites, which we here denote as the A-site (for GTP hydrolysis in SRα or FtsY) and the B-site (for SRP54 or Ffh) (Figs. 6a and S4). Although GTPase activity is stimulated upon TC formation and no stable complex can be formed *in vitro* in any SRP system, hydrolysis has been shown in bacteria to be further accelerated by the presence of SRP RNA [39]. Structural and biochemical analyses of bacterial SRP in "activated" complexes with FtsY revealed that the distal site of SRP RNA provides a catalytic nucleotide (G83 in *E. coli* [20]) to the composite active center of the TC that is defined here as the A-site. Importantly, the closed and activated conformations are virtually identical, underlining the structural pre-organization of the catalytic center of the TC prior to hydrolysis in contrast to other GTPases (i.e., Ras) [33].

Crystallization of the human TC was performed with full-length proteins and S domain SRP RNA. However, only the NG domains were ordered within the crystal, and the auxiliary domains and SRP RNA were degraded or too flexible. As in the structure of the activated bacterial complex [20], we find a purine nucleotide next to the protein–protein interface at the A-site, although the human heterodimer is in the ground state with bound GMPPNP (Fig. 6b). Due to the ground state, the purine is best interpreted with favorable hydrogen bonds as adenine (as part of an AMP nucleotide present in crystallization as a remnant of RNA degradation) that is sandwiched by SRα in between the invariant aromatic residue of the G2 element (Phe457 in hsSRα) and a leucine residue (Leu531). This general RNA-binding site is denoted in the following as N^{0A}-site (Table 2). Most importantly, the nucleotide locates to the end of a water-filled tunnel leading via the "auxiliary" water to the "catalytic" water molecule (Figs. 3 and S5), thus providing a link to the GMPPNP molecule bound to SRα. The tunnel is lined by the asparagine within G1, the (peptide-flipped) glycine of G3, and the ribose of the GMPPNP molecule *in trans* - – three important determinants in GTP hydrolysis [11,40].

The alignment of SRP RNAs [41] reveals a conserved di-nucleotide bulge (A231-G232 in *H. sapiens*, 5f-loop) in eukaryotes corresponding to the single bulged-out catalytic nucleotide within loop D in bacterial 4.5S RNA [20]. The two nucleotides are oriented toward the solvent as shown by a human S domain structure including the RNA-binding region of SRP68 [42]. Two bulged-out nucleotides also suggest two binding sites. In fact, in the human TC, continuous 2mFo-DFc electron density is found at an adjacent pocket within SRP54 next to the N^{0A}-site (Fig. 6c).

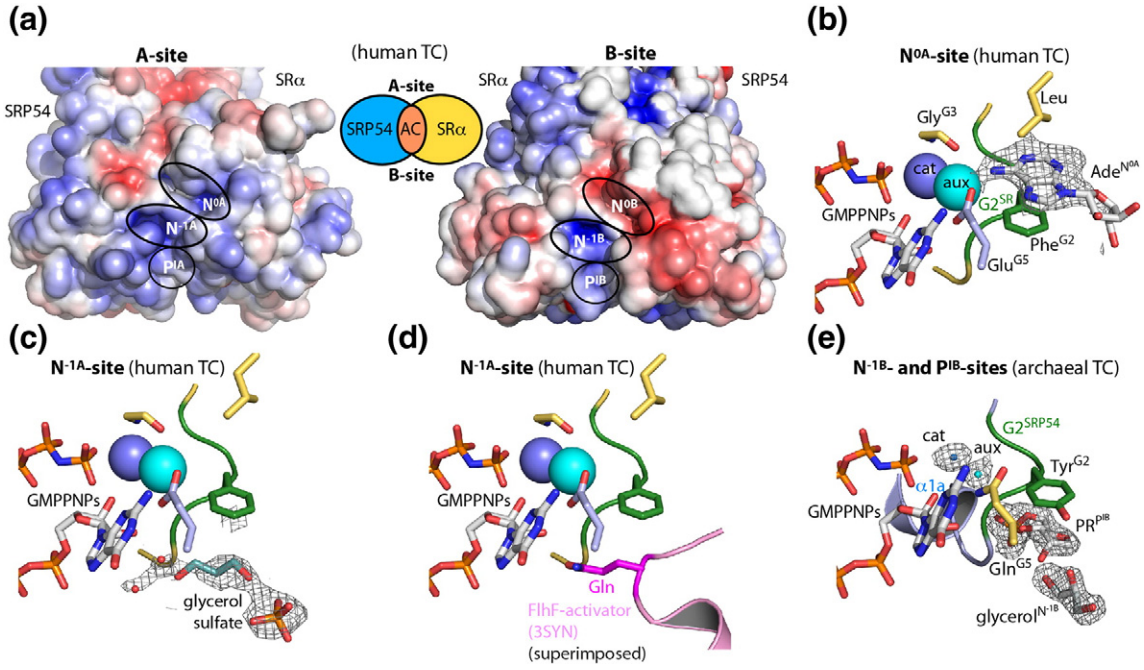

Fig. 6. External ligand-binding sites at the interface of the closed TC. (a) Electrostatic potential (±5 kT/e, blue: positive, red: negative) mapped on the surface of the human TC indicating the spatial relationship and charge distribution of external binding sites. A-sites and B-sites are classified according to the scheme (view onto the I-box as in Fig. 2). AC: active center. (b) The N^{0A}-site is sandwiched between two hydrophobic residues and locates to the end of the water-filled tunnel (aux: auxiliary, cat: catalytic) leading from the dimer interface into the active half-site of the SR (A-site). The adenosine bound to the human TC is shown with its final 2mFo-DFc map contoured at 1.0 σ. (c) The adjacent N^{-1A}-site corresponds to a pocket within SRP54 beneath the GMPPNP–ribose. Continuous electron density (0.8 σ) is modeled as sulfate, glycerol, and two water molecules but can also be explained by an AMP nucleotide. (d) A glutamine residue of the activator for the third SRP GTPase FlhF occupies the N^{-1A}-site as shown in a superposition of the activator with the human TC. (e) The B-site in the archaeal TC. The P^{IB}-site is formed by the loop connecting the G2 element and helix α1a in the I-box of SRP54 and is occupied by a glycerol. The N^{-1B} site is occupied by a glycerol.

Although the electron density is weak (0.8 σ) and has been conservatively fitted as a sulfate ion, a glycerol, and two water molecules, it could also be interpreted as an adenine nucleotide bound to this N^{-1A}-site. In the archaeal complex, a glycerol is bound in the same position as in the human complex (not shown). Strikingly, in the complex of the third SRP GTPase, FlhF with its activating protein partner, the N^{-1A}-site, is occupied by a conserved glutamine from the activator (Figs. 6d and S3B). This supports the idea of a conserved activation site [43] and a general mechanism of activation irrespective of whether it is exerted via RNA or protein. Therefore, in an activated human TC, both nucleotides of the AG-bulge could be

Table 2. Ligands of TC structures

	S. solfataricus	*H. sapiens*	*A. thaliana CP*	*T. aquaticus*	*T. aquaticus*
PDB code	this study	this study	this study	1OKK	2CNW
Active center	Mg^{2+}GMPPNP	Mg^{2+}GMPPNP	Mg^{2+}GMPPCP	Mg^{2+}GMPPCP	Mg^{2+}GDP/AlF_4
N^{0A}-site*	–	adenosine	–	–	GMP
N^{-1A}-site[$]	GOL	GOL,SO_4,H_2O	–	–	–
N^{-1B}-site	GOL	–	–	EDO	–
P^{IB}-site	phosphoribose	–	–	SO_4	–
Tetraloop site[§]	–	SO_4	–	EDO	–

GMPPCP: β,γ-Methyleneguanosine 5′-triphosphate; GMPPNP: Guanylyl-imidodiphosphate; GOL: glycerol; EDO: 1,2-ethanediol; Sites are occupied with: *SRP RNA in bacteria (PDB entries: 2XXA, 4C7O); [$]Gln of FlhF-activator (PDB entry: 3SYN); [§]GNRA-tetraloop of 4.5S RNA (PDB entry: 1ZN8).

recognized with A231 occupying the N^{-1A}-site and G232 binding to the N^{0A}-site.

Corresponding binding sites are also found on the backside of the heterodimer (at the B-site; Fig. 6a). The surrounding of the N^{0B}-site is rather negatively charged due to adjacent glutamate residues (Glu198 and Glu204 in hsSRP54). However, the hydrophobic platform comprising the aromatic G2 residue and the opposing leucine residue is conserved as in the N^{0A}-site (not shown). The N^{-1B}-site is positively charged as the N^{-1A}-site and is also occupied by a glycerol molecule in the archaeal structure (Fig. 6e). Moreover, the structure of the archaeal TC reveals density for a phosphoribose (PR) of an external GMPPNP nucleotide (present in crystallization) with the phosphate accommodated in a loop within the I-box between the G2 element and helix α1a (P^{IB}-site, for phosphate bound to I-box on B-site; Figs. 2a and 6e). The nucleotide could be directly linked to a nucleotide positioned in the N^{-1B}-site. However, if this P^{IB}-site corresponds to a nucleotide-binding site remains an open question, as the nucleobase is not bound to the surface and thus is not defined. Both P^{I}-sites might as well serve as binding sites for hydrolyzed phosphates (see below) as they are directly linked via water-filled tunnels to the γ-phosphates *in cis* (Fig. S5).

Taken together, our structural analyses suggest that the activation of the TC by SRP RNA on the A-site follows a conserved mechanism and also might occur on the B-site with another (RNA-) activator. The A- and B-sites each comprise two adjacent nucleotide-binding sites that might be occupied in the context of the SRP–RNC complex.

A universal conformational switch within the I-box

The phosphate-binding site in the I-box harboring the PR moiety in the archaeal TC is formed by the loop at the beginning of the I-box (in the following denoted P^{I}-loop for "phosphate-binding loop of the I-box"; previously also named insertion-box domain loop). The I-box is a characteristic feature of SRP GTPases (Fig. 2a, left panel) and has been described as an in-built guanine nucleotide exchange factor [44]. The P^{I}-loop comprises the G2 element and the N-terminal turn of helix α1a that are critically involved in γ-phosphate and magnesium binding [45]. The structural comparison of the archaeal TC with the individual NG domains in their GDP-bound states (Table S4 and Fig. 7) reveals that the P^{I}-loop directly responds to the presence of the magnesium ion by unwinding the first turn of helix α1a (Fig. 8a, middle and right panels). The unwinding correlates with a peptide flip of the residue directly following the G2 element (Pro137 of ssSRP54, Ala214 of ssFtsY). Interestingly, mutation of this residue to tryptophan in FtsY causes the most severe, deleterious effect on GTP hydrolysis in the bacterial system [46], which can be explained by the incompatibility of the bulky side chain with the peptide-flip mechanism. Without magnesium, this residue forms the N terminus of

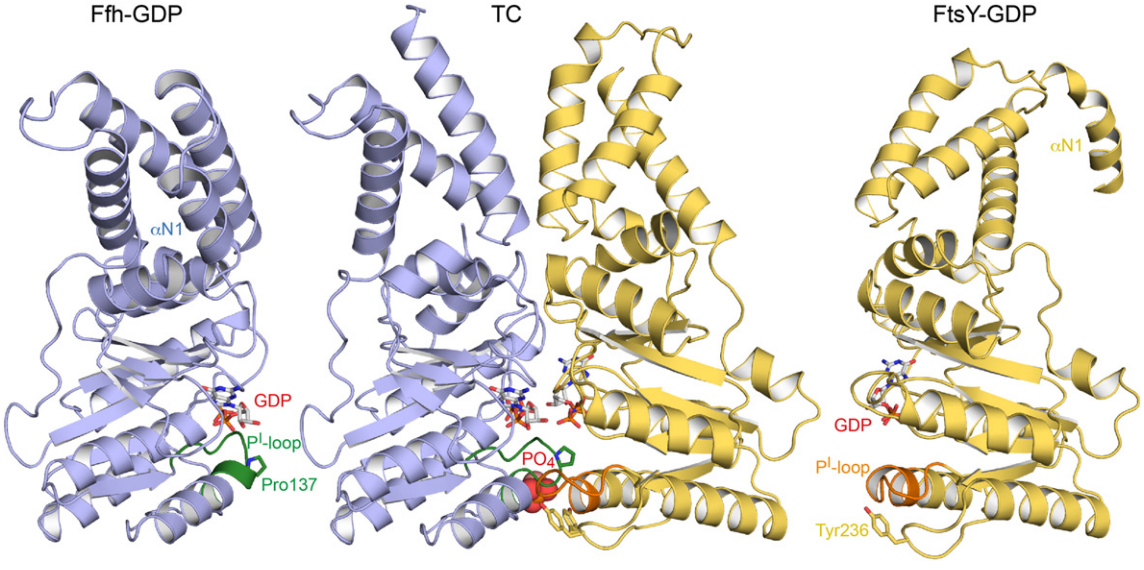

Fig. 7. SRP GTPases in the GDP-bound state. Left: Structure of archaeal Ffh from *S. solfataricus* with bound GDP. The closed P^{I}-loop with the magnesium-responding proline residue next to the GDP is highlighted in green. Helix αN1 completes the four-helix bundle of the N domain. Middle: The archaeal TC structure in the same orientation and coloring. A phosphate occupies the P^{IB}-site in the opened P^{I}-loop. Right: Structure of archaeal FtsY with bound GDP. The closed P^{I}-loop next to the GDP is highlighted in orange. The tyrosine from the proximate I-box loop occupying the P^{IA}-site in the TC structure is shown as sticks. Helix αN1 is found outside the helix-bundle of the N domain.

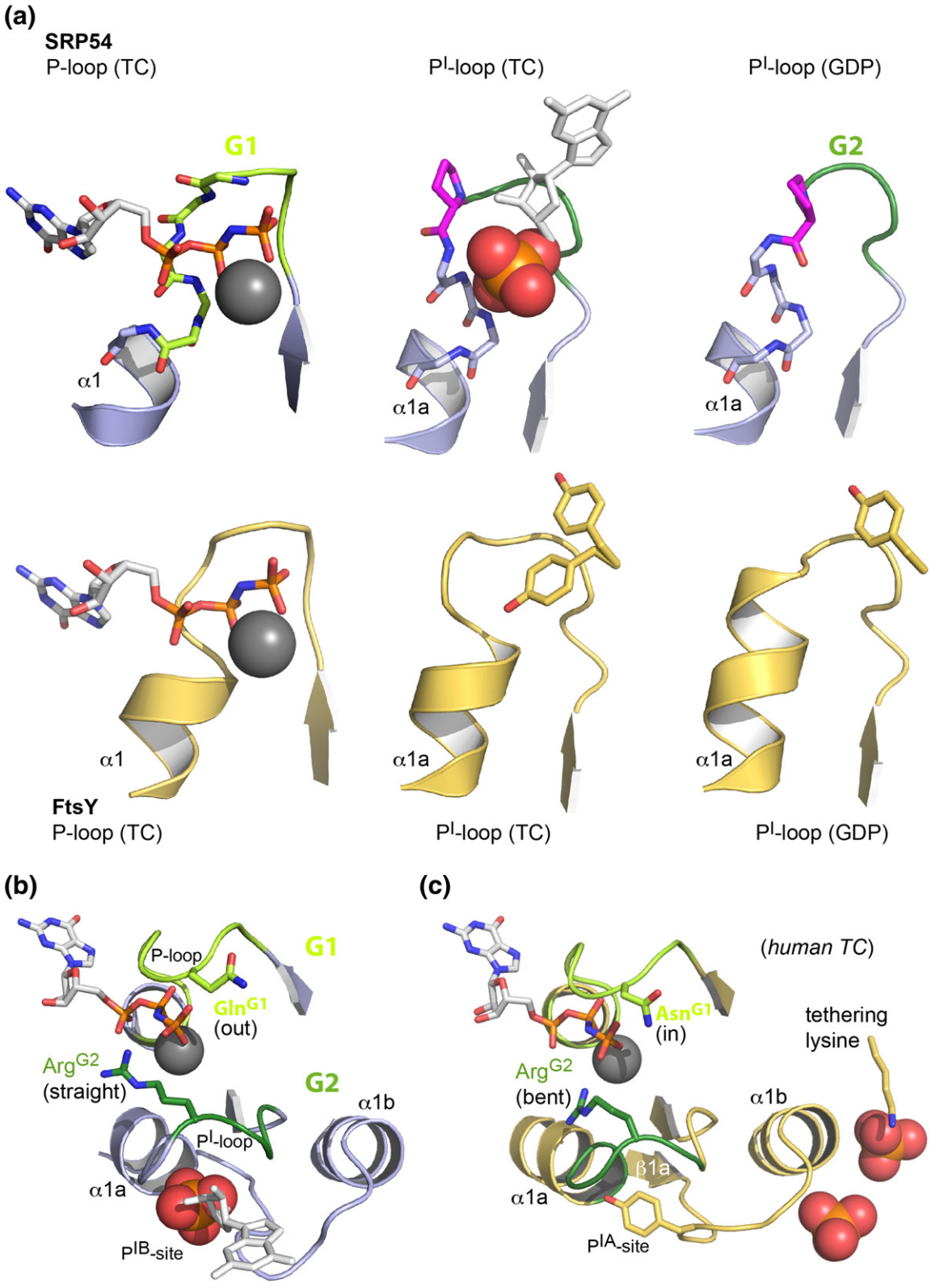

Fig. 8. (*legend on next page*)

helix α1a, and the adjacent G2 arginine relaxes into the active site (not shown). In the presence of magnesium (and also γ-phosphate), the arginine is displaced toward helix α1a and is tied to the flipped carbonyl. Helix unwinding creates an "anion hole" reminiscent of the classical P-loop structure [47] (Fig. 8a, left panels). The anion hole accommodates the phosphate of the PR moiety (Fig. 8a, top middle panel and B). The phosphate-binding pocket only exists in the presence of magnesium and concurrent nucleotide binding, and thus, it forms an inducible P-loop. Importantly, this induced fit is found in all SRP GTPase structures determined to date regardless of their origin. The induced fit is further corroborated for *E. coli* FtsY by previous hydrogen–deuterium exchange mass spectrometry analyses in solution showing a distinct backbone protection of the P^{I}-loop in the GTP- and GMPPNP-bound states *versus* the apo and GDP-bound states [29].

The general conservation of the P^{I}-loop switch raises a question about the occupation of the induced P^{IA}-site in FtsY/SRα. In contrast to the P^{IB}-site, the P^{IA}-site does not bind ligands in any TC structure and is occupied by a tyrosine residue in the human and archaeal TCs (Figs. 7 and 8a, lower middle panel). The tyrosine is flexible and adopts alternative side-chain conformations in the context of the archaeal TC. However, in the FtsY–GDP structure, it is fixed outside the closed P^{I}-loop. The tyrosine is provided by a proximal loop within the I-box connecting strand β1a and helix α1b, as shown for the human TC (Fig. 8c). The plasticity of this proximal loop is a general phenomenon observed in all co-translational SRP systems. Notably, the SRP RNA-binding region is directly on the backside of this loop, and thus, a direct communication to the active center is established (Fig. 8c).

Discussion

SRP-mediated protein targeting is controlled by the unique TC interaction of two homologous SRP GTPases of SRP and its receptor. The regulation of TC formation and GTP hydrolysis is fundamental for efficient protein translocation. Our comprehensive structural analyses provide a baseline dataset for all domains of life and show that the architecture of the TC and its catalytic machinery is highly preserved. Nonetheless, TC formation and activation of GTP hydrolysis have been evolutionarily adapted. The formation of the early intermediate is structurally validated only for the bacterial system [10]. The conservation of surface charge patterns together with our computational and biochemical studies for the archaeal system suggests the formation of this intermediate, facilitated by N domain electrostatic complementarity, for all SRP RNA-containing systems. Chloroplast TC formation in higher plants might follow a different strategy, as the receptor FtsY, in particular, is already structurally primed for the GTP-dependent closed TC conformation. The electrostatic potential of chloroplast TC is distinct, and the SRP RNA-binding surface is not preserved, as reflected by the absence of SRP RNA in higher plants. The pronounced surface charge distribution of the chloroplast TC might support ribosome binding in the co-translational mode and membrane insertase binding in the post-translational mode.

The GTPase switch cycle of SRP GTPases is unique as two GTP molecules are in direct contact in the interface of the closed TC. Enclosure of the nucleotides assembles the composite active center including the G1 to G5 elements and the built-in arginine finger for stabilization of the transition state. The closed TC is ready to activate and can hydrolyze GTP spontaneously *in vitro*. However, for faithful protein targeting *in vivo*, activation needs to be coordinated with signal sequence release. TC closure already seems to occur at the proximal SRP RNA site as seen for the bacterial system [20]. Apparently, hydrolysis in this position is still inhibited by the presence of the RNC and/or the absence of an external activator.

Based on the conservation of the active center and of external nucleotide-binding sites in all TCs, we propose the following general scenario for RNA activation: closure leads to displacement of the TC from the tetraloop and the ribosomal surface to the distal site of SRP RNA. This relocation, enforced by the translocation channel as shown by FRET studies [14], changes the physicochemical environment at the A-site. In particular, the nucleotide in the N^{0A}-site buries the invariant glutamate in the G5 element (Glu^{G5}, Fig. 6b). In the activated TC, as in the structure for the bacterial system, the nucleotide

Fig. 8. The inducible P^{I}-loop in the I-box. (a) Left: The classical P-loop in the archaeal TC. The β-phosphates of the nucleotides are accommodated in a pocket formed by the main chain nitrogens of the P-loop (only shown for SRP54) and the N terminus of the following helix. The G1 element is shown in light green and the magnesium ion as a gray sphere. Middle: The P^{I}-loop in the TC forms an equivalent structure and in SRP54 constitutes the P^{IB}-site that is occupied by the phosphate (spheres) of an external GMPPNP molecule (sticks). The G2 element is shown in dark green and the flipping peptide bond (proline) in magenta. Right: The P^{I}-loop in the individual GDP-structures without magnesium. The peptide is flipped and helix α1a is prolonged by one turn. The P^{I}-loop is closed. (b) Spatial relation of the P^{IB}-loop and the active center shown for SRP54 of the archaeal TC. Conserved asymmetries within the active center are indicated. (c) Spatial relation of SRP RNA-binding site (indicated by bound sulfates for the tetraloop), the P^{IA}-loop, and the active center shown for SRα of the human TC.

corresponds to a bulged-out single guanine within loop D of SRP RNA [20]. To date, there is only one archaeal structure that includes the distal site (from *Methanococcus jannaschii* [48]). Here, a single guanine corresponding to *E. coli* G83 is bulged out from SRP RNA. Thus, we conclude that in most prokaryotes, the activation might occur in a similar fashion.

For eukaryotes, and especially mammalian SRP, activation of the TC appears more sophisticated. In a previously determined cryo-EM structure of mammalian SRP-SR bound to an RNC [13], electron density at the distal site can be interpreted as activated TC bound to SRP RNA (Fig. 9a). Binding of SRP RNA to the N^{0A}-site of the TC matches with G232 of the AG-bulge in eukaryotic SRP (Fig. 9b) [42]. The adjacent A231 could then occupy the N^{-1A}-site as supported by the human TC structure. SRP RNA binds only to the A-site and thus induces asymmetry at the TC, suggestive of sequential hydrolysis events first occurring in the SR and then in SRP54/Ffh. Whether (ribosomal) RNA on the B-site accelerates hydrolysis within SRP54/Ffh remains to be elucidated.

Finally, if SRP GTPase activation by RNA is a general principle, how is it then performed in the chloroplast system lacking SRP RNA? In the co-translational targeting mode, the pronounced positively charged surface pattern might establish a direct contact with ribosomal RNA, possibly substituting for SRP RNA. However, RNA-independent activation has been described for the third (homodimeric) SRP GTPase FlhF involved in flagella assembly [43]. Here, an activating protein inserts a catalytic residue into a pocket that corresponds to the N^{-1A}-site. Thus, activation by RNA is not an exclusive mechanism for SRP GTPases, and a similar mode of protein-driven activation—potentially also by SRP43 in the post-translational targeting mode—might apply to the chloroplast SRP system.

Taken together, our survey of the structures and binding sites of TCs covers all domains of life and allows generalization and differentiation of mechanistic paradigms. However, no complete series of snapshots for the GTPase cycle is available for any main phylogenetic branch, and the limited number of investigated systems still leaves room for further surprises.

Materials and methods

Cloning and protein expression

Gene fragments encoding residues 71–369 of crenarchaeal FtsY and residues 1–291 of *S. solfataricus* SRP54 and for cpSRP54 and cpFtsY from *A. thaliana* (residues 77–371 and 80–366, respectively) were amplified by polymerase chain reaction using the Expand High Fidelity PCR system (Roche) and cloned into pET24d vector (Novagen) via the NcoI/BamHI restriction sites. Cells were grown in lysogeny broth medium (LB) complemented with 1.5% (wt/vol) D(+)-lactose monohydrate for 16 h at 30 °C. DNA was

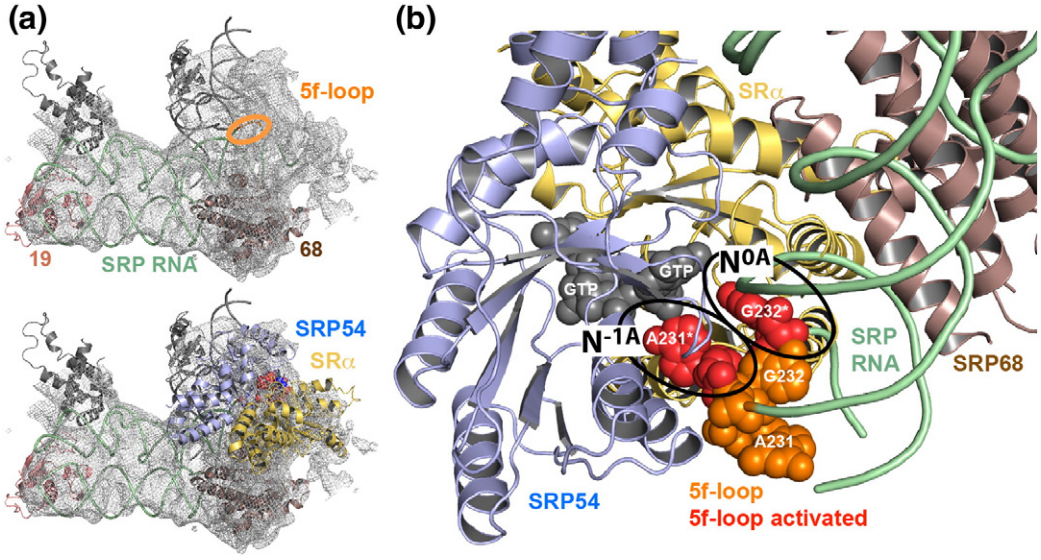

Fig. 9. Model for activation of the human TC by RNA. (a) Interpretation and placement of an activated TC in the cryo-EM density for the eukaryotic SRP–SR/RNC complex [13]. Upper panel: View on the ribosomal tunnel exit. SRP components are colored and labeled. The position of the distal 5f-loop is indicated. Ribosomal contacts are shown in gray. Lower panel: Same view with modeled human TC. (b) Model for human TC bound to the 5f-loop of SRP RNA. The two nucleotides A231 and G232 of the 5f-loop are bulged out [42] (orange) and overlap with the two external nucleotides placed in the N^{0A}- and N^{-1A}-sites (red).

mutated by the QuikChange site-directed mutagenesis kit (Stratagene) following the procedure described in the manufacturer's manual.

The gene encoding residues 1–436 of *Canis familiaris* SRP54 was cloned into the pET-24d vector (Novagen) using the Nco1/Xho1 sites with an N-terminal hexa-histidine tag. The genes encoding full-length human SRα and *Mus musculus* SRβ lacking the transmembrane anchor (residues 58–271) were bi-cistronically cloned into the pET-16b vector between the Nco1/BamH1 sites. SRP54 from *C. familiaris* and *M. musculus* SRβ are identical to the human proteins. The eukaryotic TC (*cf*SRP54/*hs*SRα) is therefore termed human TC. SRP19 and SRP RNA (nucleotides 123–227) constructs from *H. sapiens* were produced as described previously [49].

Protein purification and complex formation

S. solfataricus TC

Cell pellets were resuspended in 20 mM Hepes (pH 8.0), 250 mM NaCl, 10 mM $MgCl_2$, and 10 mM KCl and passed through an M-110 L Microfluidizer (Microfluidics). The lysate was clarified by ultra-centrifugation (125,000 x g for 30 min at 277 K), and the supernatant was applied onto a HighTrap column (GE Healthcare) and eluted in lysis buffer with a step gradient of 40 mM and 500 mM imidazole. The protein was concentrated to 30 mg/ml and purified via size-exclusion chromatography (S75/26-60, GE Healthcare) in a buffer consisting of 20 mM Hepes (pH 7.5), 150 mM NaCl, 10 mM $MgCl_2$, and 10 mM KCl. Equal amounts of SRP54 and FtsY were incubated together in the presence of 2 mM GMPPNP at 65 °C for 2 h to reconstitute the SRP54/FtsY heterodimer. Unbound protein or nucleotide was removed by size-exclusion chromatography (S75/26-60, GE Healthcare) in the same buffer as above.

For the *in vitro* validation of the effects on target complex formation, the mutant proteins were purified as the wild-type proteins. Equal amounts of SRP54 and FtsY were then mixed and incubated at 65 °C in the presence of 2 mM GMPPNP. Every 30 min, an aliquot was taken and analyzed by size-exclusion chromatography.

A. thaliana TC

The NG domains of cpSRP54 and cpFtsY were purified as described for their counterparts from *S. solfataricus* (see above). After size-exclusion chromatography, equal amounts of cpSRP54 and cpFtsY were incubated together in the presence of 2 mM GMPPCP at 37 °C for 30 min to reconstitute the chloroplast TC.

H. sapiens TC

The human TC was reconstituted from full-length proteins (SRP54 and SRα) and the S domain SRP RNA in context of a pentameric assembly (105 nts of SRP RNA, SRP19, SRP54, and SRαβ). Briefly, the binary SRP19/SRP RNA complex and the SRαβ complex were over-expressed and purified as previously described [49]. SRP54 was purified basically as described for the archaeal NG domain. Complex formation was done in a buffer consisting of 20 mM Tris–Cl (pH 8.0), 250 mM NaCl, 10 mM $MgCl_2$, and 10 mM KCl at 37 °C in the presence of 3 mM GMPPNP and was subsequently purified by size-exclusion chromatography (S200/16–60, GE Healthcare).

Crystallization, structure determination, and refinement

S. solfataricus TC

Crystals were grown by the hanging drop method. For initial trials, equal volumes (1–2 µl) of protein solution (10 mg/ml) and crystallization screening buffer were mixed on a cover slip and suspended over a reservoir containing 1 ml crystallization screening solution. All experiments were performed at 20 °C. Archaeal complex crystallized within 1–7 days in a buffer containing 0.1 M Mes (pH 5.8) and 1.26 M ammonium sulfate. Crystals were flash-cooled with 30% (vol/vol) glycerol as cryo-protectant. Diffraction data were collected at the European Synchrotron Radiation Facility (ESRF) in Grenoble. Data were processed with MOSFLM and SCALA [50]. The structure of the archaeal complex was determined by molecular replacement using CCP4-implemented AMoRe and the model of the bacterial ortholog from *T. aquaticus* [12].

H. sapiens TC

The human TC complex was crystallized as a degradation product of the assembled pentameric complex in an automated crystallization platform by mixing complex (8 mg/ml) with reservoir solution (3:1 ratio) consisting of 100 mM Tris–HCl (pH 8.0), 400 mM lithium sulfate, and 10% (wt/vol) polyethylene gylcol (PEG) 8000 at 4 °C. Crystals were flash-cooled with 20% (vol/vol) glycerol as cryo-protectant. Data were collected at 100 K at the beamline ID23-1 at the ESRF (Grenoble, France) and processed using MOSFLM and SCALA [50]. The structure of the TC was determined by molecular replacement using CCP4 implemented PHASER and the *S. solfataricus* complex (this study) as start model.

A. thaliana TC

The chloroplast complex was crystallized in an automated crystallization platform by mixing complex (15 mg/ml) with reservoir solution (1:1) consisting of 0.2 M magnesium formate and 20% (wt/vol) PEG3350. Crystal typically appeared after 1 week at 18 °C. The structure of the targeting complex was determined by molecular replacement using CCP4 implemented PHASER and the *S. solfataricus* complex (this study) as start model.

All structures in this study were manually built with COOT [51] and refined and analyzed with PHENIX [52]. Electrostatic potentials were calculated and mapped onto molecular surfaces using the APBS plugin in Pymol [53]. All figures were prepared with Pymol.

Brownian dynamics calculations

The GMPPNP-bound structures of SRP54 and FtsY from the crystal structure of the *S. solfataricus* TC were used for the calculations. Polar hydrogen atoms were added to protein residues of the archaeal GTPases and to

the GMPPNP nucleotide. Electrostatic potentials were calculated with the UHBD program [54]. The dielectric constants of the solvent and the protein were set to 78.0 and 4.0, respectively, and the ionic strength was set to 150 mM. Rigid-body protein–protein docking was performed with a modified version of the SDA [55] program that employs a Brownian Dynamics algorithm to simulate protein–protein association. Effective charges were calculated with the ECM program [56]. The simulations were run for 100 μs with the RMSD filtering option set to 1.0 Å and a biasing energy of −4 kT. Distance constraints were applied between the PG and O3′ atoms of the GMPPNP molecules of SRP54 and FtsY with different thresholds, namely 10, 12, 14, 16, 18, and 20 Å. In total, 500 docked structures of FtsY were recorded that satisfied the distance constraints, and these were clustered with a hierarchical clustering algorithm [57]. The following metrics were used to evaluate the clusters: average electrostatic interaction energy of the cluster as calculated by SDA, the average backbone RMSD of the cluster members with respect to FtsY in its orientation in the crystal structure of the bound complex, and the spread of the clusters calculated as an average backbone RMSD from a structure in the middle of the cluster to every other structure of the cluster.

The putative effects on complexation of mutated residues were estimated using HyPare [58], which allows the prediction of "hot-spot" residues with strong effects on the association rates upon charge mutation. Selected residues were mutated *in silico* into alanines or to residues with opposite charge, and the electrostatic potentials of the mutant proteins were recalculated with UHBD [54]. Docking simulations were then performed with the alanine mutants with a loose distance constraint of 18 Å between the nucleotides.

Accession numbers

Coordinates and structure files have been deposited at the Protein Data Bank (PDB) with accession numbers: 5L3Q (human TC), 5L3S (archaeal TC), 5L3R (chloroplast TC), 5L3V (archaeal SRP54-GDP), and 5L3W(archaeal FtsY-GDP).

Acknowledgments

We thank Ralf Moll (University of Lübeck) for the genomic DNA of *S. solfataricus*, Ken R. Rosendal and Gunes Bozkurt for their contribution at the beginning of the project, and Musa Özboyaci (HITS) for assistance with figure preparation. This work was supported by the Deutsche Forschungsgemeinschaft (SFB638, GRK1188 to I.S.) and the Klaus Tschira Foundation (D.M. and R.C.W.). G.B. thanks the Peter and Traudl Engelhorn Foundation for financial support. We thank Jürgen Kopp and Claudia Siegmann from the BZH/Cluster of Excellence:CellNetworks crystallization platform. We acknowledge access to the beamlines at the ESRF in Grenoble and the support of the beamline scientists.

The authors declare no financial conflict of interest.

Appendix A. Supplementary Data

Supplementary data to this article can be found online at http://dx.doi.org/10.1016/j.jmb.2016.05.015.

Received 18 March 2016;
Received in revised form 13 May 2016;
Accepted 18 May 2016
Available online 27 May 2016

Keywords:
co-translational protein targeting;
ribonucleoprotein complex;
SRP GTPase;
X-ray structure analysis;
molecular modeling

†K.W. and G.B. contributed equally to this work.

Present address: G. Bange, LOEWE Center for Synthetic Microbiology (SYNMIKRO) & Faculty of Chemistry, Phillips University Marburg, Hans-Meerwein-Straße C7, D-35043 Marburg, Germany.
Present address: D. Motiejunas, Life Technologies, Gaston Crommenlaan 4, 9050, Ghent, Belgium.

Abbreviations used:
SRP, signal recognition particle; RNCs, ribosome–nascent chain complexes; TC, targeting complex; cryo-EM, cryo-electron microscopy; FRET, fluorescence resonance energy transfer; GMPPNP, 5′-Guanylyl-imidodiphosphate; GMPPCP, β,γ-Methyleneguanosine 5′-triphosphate; nts, nucleotides; MTS, membrane targeting sequence; PR, phosphoribose; ESRF, European synchrotron radiation facility.

References

[1] M.M. Elvekrog, P. Walter, Dynamics of co-translational protein targeting, Curr. Opin. Chem. Biol. 29 (2015) 79–86.
[2] P. Grudnik, G. Bange, I. Sinning, Protein targeting by the signal recognition particle, Biol. Chem. 390 (2009) 775–782.
[3] G. Bange, I. Sinning, SIMIBI twins in protein targeting and localization, Nat. Struct. Mol. Biol. 20 (2013) 776–780.
[4] D.D. Leipe, Y.I. Wolf, E.V. Koonin, L. Aravind, Classification and evolution of P-loop GTPases and related ATPases, J. Mol. Biol. 317 (2002) 41–72.
[5] R. Gasper, S. Meyer, K. Gotthardt, M. Sirajuddin, A. Wittinghofer, It takes two to tango: regulation of G proteins by dimerization, Nat. Rev. Mol. Cell Biol. 10 (2009) 423–429.
[6] T.S. Murray, B.I. Kazmierczak, FlhF is required for swimming and swarming in *Pseudomonas Aeruginosa*, J. Bacteriol. 188 (2006) 6995–7004.
[7] P.J. Rapiejko, R. Gilmore, Empty site forms of the SRP54 and SR alpha GTPases mediate targeting of ribosome-nascent chain complexes to the endoplasmic reticulum, Cell 89 (1997) 703–713.

[8] G. Montoya, C. Svensson, J. Luirink, I. Sinning, Crystal structure of the NG domain from the signal-recognition particle receptor FtsY, Nature. 385 (1997) 365–368.
[9] D.M. Freymann, R.J. Keenan, R.M. Stroud, P. Walter, Structure of the conserved GTPase domain of the signal recognition particle, Nature. 385 (1997) 361–364.
[10] L.F. Estrozi, D. Boehringer, S.O. Shan, N. Ban, C. Schaffitzel, Cryo-EM structure of the *E. coli* translating ribosome in complex with SRP and its receptor, Nat. Struct. Mol. Biol. 18 (2011) 88–90.
[11] P.F. Egea, S.O. Shan, J. Napetschnig, D.F. Savage, P. Walter, R.M. Stroud, Substrate twinning activates the signal recognition particle and its receptor, Nature 427 (2004) 215–221.
[12] P.J. Focia, I.V. Shepotinovskaya, J.A. Seidler, D.M. Freymann, Heterodimeric GTPase core of the SRP targeting complex, Science 303 (2004) 373–377.
[13] M. Halic, M. Gartmann, O. Schlenker, T. Mielke, M.R. Pool, I. Sinning, et al., Signal recognition particle receptor exposes the ribosomal translocon binding site, Science. 312 (2006) 745–747.
[14] K. Shen, S. Arslan, D. Akopian, T. Ha, S.O. Shan, Activated GTPase movement on an RNA scaffold drives co-translational protein targeting, Nature 492 (2012) 271–275.
[15] P. Kuhn, A. Draycheva, A. Vogt, N.A. Petriman, L. Sturm, F. Drepper, et al., Ribosome binding induces repositioning of the signal recognition particle receptor on the translocon, J. Cell Biol. 211 (2015) 91–104.
[16] A. Jomaa, D. Boehringer, M. Leibundgut, B. N, Structures of the *E. coli* translating ribosome with SRP and its receptor and with the translocon, Nat. Commun. 7 (2016) 10,471.
[17] O. von Loeffelholz, Q. Jiang, A. Ariosa, M. Karuppasamy, K. Huard, I. Berger, et al., Ribosome–SRP–FtsY cotranslational targeting complex in the closed state, Proc. Natl. Acad. Sci. U. S. A. 112 (2015) 3943–3948.
[18] R.M. Voorhees, T.M. Schmeing, A.C. Kelley, V. Ramakrishnan, The mechanism for activation of GTP hydrolysis on the ribosome, Science. 330 (2010) 835–838.
[19] S.F. Ataide, N. Schmitz, K. Shen, A. Ke, S.O. Shan, J.A. Doudna, et al., The crystal structure of the signal recognition particle in complex with its receptor, Science. 331 (2011) 881–886.
[20] F. Voigts-Hoffmann, N. Schmitz, K. Shen, S.O. Shan, S.F. Ataide, N. Ban, The structural basis of FtsY recruitment and GTPase activation by SRP RNA, Mol. Cell. 52 (2013) 643–654.
[21] P.F. Egea, H. Tsuruta, G.P. de Leon, J. Napetschnig, P. Walter, R.M. Stroud, Structures of the signal recognition particle receptor from the archaeon *Pyrococcus furiosus*: implications for the targeting step at the membrane, PLoS ONE. 3 (2008), e3619.
[22] M.A. Rosenblad, N. Larsen, T. Samuelsson, C. Zwieb, Kinship in the SRP RNA family, RNA Biol. 6 (2009) 508–516.
[23] C. Trager, M.A. Rosenblad, D. Ziehe, C. Garcia-Petit, L. Schrader, K. Kock, et al., Evolution from the prokaryotic to the higher plant chloroplast signal recognition particle: the signal recognition particle RNA is conserved in plastids of a wide range of photosynthetic organisms, Plant Cell 24 (2012) 4819–4836.
[24] M. Halic, M. Blau, T. Becker, T. Mielke, M.R. Pool, K. Wild, et al., Following the signal sequence from ribosomal tunnel exit to signal recognition particle, Nature 444 (2006) 507–511.
[25] K.R. Rosendal, K. Wild, G. Montoya, I. Sinning, Crystal structure of the complete core of archaeal signal recognition particle and implications for interdomain communication, Proc. Natl. Acad. Sci. U. S. A. 100 (2003) 14,701–14,706.
[26] K. Wild, M. Halic, I. Sinning, R. Beckmann, SRP meets the ribosome, Nat. Struct. Mol. Biol. 11 (2004) 1049–1053.
[27] R. Parlitz, A. Eitan, G. Stjepanovic, L. Bahari, G. Bange, E. Bibi, et al., *Escherichia coli* signal recognition particle receptor FtsY contains an essential and autonomous membrane-binding amphipathic helix, J. Biol. Chem. 282 (2007) 32,176–32,184.
[28] K.F. Stengel, I. Holdermann, K. Wild, I. Sinning, The structure of the chloroplast signal recognition particle (SRP) receptor reveals mechanistic details of SRP GTPase activation and a conserved membrane targeting site, FEBS Lett. 581 (2007) 5671–5676.
[29] G. Stjepanovic, K. Kapp, G. Bange, C. Graf, R. Parlitz, K. Wild, et al., Lipids trigger a conformational switch that regulates signal recognition particle (SRP)-mediated protein targeting, J. Biol. Chem. 286 (2011) 23,489–23,497.
[30] B. Jadhav, K. Wild, M.R. Pool, I. Sinning, Structure and switch cycle of SRbeta as ancestral eukaryotic GTPase associated with secretory membranes, Structure 23 (2015) 1838–1847.
[31] K. Wild, K.R. Rosendal, I. Sinning, A structural step into the SRP cycle, Mol. Microbiol. 53 (2004) 357–363.
[32] G. Bange, G. Petzold, K. Wild, R.O. Parlitz, I. Sinning, The crystal structure of the third signal-recognition particle GTPase FlhF reveals a homodimer with bound GTP, Proc. Natl. Acad. Sci. U. S. A. 104 (2007) 13,621–13,625.
[33] M.R. Ahmadian, P. Stege, K. Scheffzek, A. Wittinghofer, Confirmation of the arginine-finger hypothesis for the GAP-stimulated GTP-hydrolysis reaction of Ras, Nat. Struct. Biol. 4 (1997) 686–689.
[34] X. Zhang, V.Q. Lam, Y. Mou, T. Kimura, J. Chung, S. Chandrasekar, et al., Direct visualization reveals dynamics of a transient intermediate during protein assembly, Proc. Natl. Acad. Sci. U. S. A. 108 (2011) 6450–6455.
[35] K. Shen, S.O. Shan, Transient tether between the SRP RNA and SRP receptor ensures efficient cargo delivery during cotranslational protein targeting, Proc. Natl. Acad. Sci. U. S. A. 107 (2010) 7698–7703.
[36] K.F. Stengel, I. Holdermann, P. Cain, C. Robinson, K. Wild, I. Sinning, Structural basis for specific substrate recognition by the chloroplast signal recognition particle protein cpSRP43, Science 321 (2008) 253–256.
[37] P. Jaru-Ampornpan, S. Chandrasekar, S.O. Shan, Efficient interaction between two GTPases allows the chloroplast SRP pathway to bypass the requirement for an SRP RNA, Mol. Biol. Cell 18 (2007) 2636–2645.
[38] K. Shen, Y. Wang, Y.H. Hwang Fu, Q. Zhang, J. Feigon, S.O. Shan, Molecular mechanism of GTPase activation at the SRP RNA distal end, J. Biol. Chem. 288 (2013) 36,385–36,397.
[39] P. Peluso, S.O. Shan, S. Nock, D. Herschlag, P. Walter, Role of SRP RNA in the GTPase cycles of Ffh and FtsY, Biochemistry 40 (2001) 15,224–15,233.
[40] M.J. Yang, X.Q. Pang, X. Zhang, K.L. Han, Molecular dynamics simulation reveals preorganization of the chloroplast FtsY toward complex formation induced by GTP binding, J. Struct. Biol. 173 (2011) 57–66.
[41] M.A. Rosenblad, J. Gorodkin, B. Knudsen, C. Zwieb, T. Samuelsson, SRPDB: signal recognition particle database, Nucleic Acids Res. 31 (2003) 363–364.

[42] J.T. Grotwinkel, K. Wild, B. Segnitz, I. Sinning, SRP RNA remodeling by SRP68 explains its role in protein translocation, Science 344 (2014) 101–104.
[43] G. Bange, N. Kummerer, P. Grudnik, R. Lindner, G. Petzold, D. Kressler, et al., Structural basis for the molecular evolution of SRP-GTPase activation by protein, Nat. Struct. Mol. Biol. 18 (2011) 1376–1380.
[44] C. Moser, O. Mol, R.S. Goody, I. Sinning, The signal recognition particle receptor of *Escherichia coli* (FtsY) has a nucleotide exchange factor built into the GTPase domain, Proc. Natl. Acad. Sci. U. S. A. 94 (1997) 11,339–11,344.
[45] I. Saraogi, S.O. Shan, Molecular mechanism of co-translational protein targeting by the signal recognition particle, Traffic 12 (2011) 535–542.
[46] S.O. Shan, S. Chandrasekar, P. Walter, Conformational changes in the GTPase modules of the signal reception particle and its receptor drive initiation of protein translocation, J. Cell Biol. 178 (2007) 611–620.
[47] D. Dreusicke, G.E. Schulz, The glycine-rich loop of adenylate kinase forms a giant anion hole, FEBS Lett. 208 (1986) 301–304.
[48] T. Hainzl, S. Huang, G. Merilainen, K. Brannstrom, A.E. Sauer-Eriksson, Structural basis of signal-sequence recognition by the signal recognition particle, Nat. Struct. Mol. Biol. 18 (2011) 389–391.
[49] K. Wild, G. Bange, G. Bozkurt, B. Segnitz, A. Hendricks, I. Sinning, Structural insights into the assembly of the human and archaeal signal recognition particles, Acta Crystallogr. D Biol. Crystallogr. 66 (2010) 295–303.
[50] M.D. Winn, C.C. Ballard, K.D. Cowtan, E.J. Dodson, P. Emsley, P.R. Evans, et al., Overview of the CCP4 suite and current developments, Acta Crystallogr. D Biol. Crystallogr. 67 (2011) 235–242.
[51] P. Emsley, K. Cowtan, Coot: model-building tools for molecular graphics, Acta Crystallogr. D Biol. Crystallogr. 60 (2004) 2126–2132.
[52] P.H. Zwart, P.V. Afonine, R.W. Grosse-Kunstleve, L.W. Hung, T.R. Ioerger, A.J. McCoy, et al., Automated structure solution with the PHENIX suite, Methods Mol. Biol. 426 (2008) 419–435.
[53] L.L.C. Schrodinger, The PyMOL Molecular Graphics System, Version 1.8, 2015.
[54] J.D. Madura, J.M. Briggs, R.C. Wade, M.E. Davis, B.A. Luty, A. Ilin, et al., Electostatics and diffusion of molecules in solution: simulations with the university of Houston brownian dynamics program, Comput. Phys. Commun. 91 (1995) 57–95.
[55] R.R. Gabdoulline, R.C. Wade, Brownian dynamics simulation of protein–protein diffusional encounter, Methods 14 (1998) 329–341.
[56] R.R. Gabdoulline, R.C. Wade, Effective charges for macromolecules in solvent, J. Phys. Chem. 100 (1996) 3868–3878.
[57] D. Motiejunas, R. Gabdoulline, T. Wang, A. Feldman-Salit, T. Johann, P.J. Winn, et al., Protein–protein docking by simulating the process of association subject to biochemical constraints, Proteins 71 (2008) 1955–1969.
[58] G. Schreiber, Y. Shaul, K.E. Gottschalk, Electrostatic design of protein–protein association rates, Methods Mol. Biol. 340 (2006) 235–249.